Chemical Research in Toxicology

ARTICLE

pubs.acs.org/crt

One-Electron Reduction of *N*-Chlorinated and *N*-Brominated Species Is a Source of Radicals and Bromine Atom Formation

David I. Pattison,*[,†,∥] Robert J. O'Reilly,[‡] Ojia Skaff,[†] Leo Radom,[‡] Robert F. Anderson,[§] and Michael J. Davies[†,∥]

[†]The Heart Research Institute, 7 Eliza Street, Newtown, NSW 2042, Australia

[‡]School of Chemistry and ARC Centre of Excellence for Free Radical Chemistry and Biotechnology, University of Sydney, Sydney, NSW 2006, Australia

[§]Department of Chemistry, University of Auckland, Auckland, New Zealand

[∥]Faculty of Medicine, University of Sydney, Sydney, NSW 2006, Australia

Supporting Information

ABSTRACT: Hypochlorous (HOCl) and hypobromous (HOBr) acids are strong bactericidal oxidants that are generated by the human immune system but are implicated in the development of many human inflammatory diseases (e.g., atherosclerosis, asthma). These oxidants react readily with sulfur- and nitrogen-containing nucleophiles, with the latter generating *N*-halogenated species (e.g., chloramines/bromamines (RR′NX; X = Cl, Br)) as initial products. Redox-active metal ions and superoxide radicals ($O_2^{\bullet-}$) can reduce *N*-halogenated species to nitrogen- and carbon-centered radicals. *N*-Halogenated species and $O_2^{\bullet-}$ are generated simultaneously at sites of inflammation, but the significance of their interactions remains unclear. In the present study, rate constants for the reduction of *N*-halogenated amines, amides, and imides to model potential biological substrates have been determined. Hydrated electrons reduce these species with $k_2 > 10^9\ M^{-1}\ s^{-1}$, whereas $O_2^{\bullet-}$ reduced only *N*-halogenated imides with complex kinetics indicative of chain reactions. For *N*-bromoimides, heterolytic cleavage of the N−Br bond yielded bromine atoms ($Br^{\bullet}$), whereas for other substrates, *N*-centered radicals and Cl^-/Br^- were produced. High-level quantum chemical procedures have been used to calculate gas-phase electron affinities and aqueous solution reduction potentials. The effects of substituents on the electron affinities of aminyl, amidyl, and imidyl radicals are rationalized on the basis of differential effects on the stabilities of the radicals and anions. The calculated reduction potentials are consistent with the experimental observations, with $Br^{\bullet}$ production predicted for *N*-bromosuccinimide, while halide ion formation is predicted in all other cases. These data suggest that interaction of *N*-halogenated species with $O_2^{\bullet-}$ may produce deleterious *N*-centered radicals and $Br^{\bullet}$.

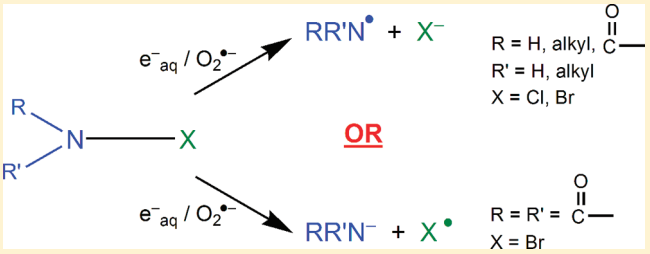

1. INTRODUCTION

A major feature of the human inflammatory response is the recruitment of phagocytic white blood cells (neutrophils, eosinophils, monocytes, or macrophages) to sites of inflammation and their subsequent activation. The latter results in a respiratory burst that consumes oxygen and generates a high flux of superoxide radicals ($O_2^{\bullet-}$) via an NADPH oxidase (NOX2) complex (reviewed in ref 1). The $O_2^{\bullet-}$ subsequently rapidly dismutates to generate hydrogen peroxide (H_2O_2) and O_2.

Simultaneous to the respiratory burst, activated leukocytes release a range of inflammatory mediators, including protease and peroxidase enzymes, from intracellular granules.[2,3] Myeloperoxidase (MPO) is a major protein component of the phagocytic granules of neutrophils, monocytes, and some tissue macrophages, while eosinophil peroxidase (EPO) is released from eosinophils.[2] These enzymes utilize the H_2O_2 generated during the respiratory burst to oxidize chloride, bromide, and thiocyanate ions to hypochlorous (HOCl), hypobromous (HOBr), and hypothiocyanous (HOSCN) acids.[2,3]

HOCl and HOBr are strong oxidants and potent antibacterial agents that react rapidly with nucleophilic targets (reviewed in ref 4); in biological systems, this is comprised primarily of sulfur- and nitrogen-containing moieties. Thus, in proteins the primary sites of attack by HOCl and HOBr are free thiols (Cys side-chain), thioethers (Met side-chain), disulfide bonds (cystine), amines (Lys side-chain), and other nitrogenous side-chains (e.g., His).[4−7] In contrast, HOSCN specifically targets thiol residues.[8−10] HOCl and HOBr also react with nitrogen-containing moieties in DNA/RNA bases, phospholipids and some polysaccharides.[4,11−15] These reactions result in halogenation of the nucleophilic nitrogen center to form *N*-halogenated species (RR′N-Cl or RR′N-Br), which retain the oxidizing

Received: September 21, 2010
Published: February 23, 2011

capacity of HOCl and HOBr but have relatively long half-lives.[16−19] The properties of *N*-halogenated species render them potentially important intermediates in the biological effects of HOCl and HOBr.[20−23]

N-Halogenated species react via multiple pathways (reviewed in refs 2 and 24), including: (i) one-electron reduction to yield radicals, (ii) halogen transfer to regenerate the parent compound, or (iii) hydrolysis (via an imine) to yield carbonyl derivatives. Of particular interest in the current studies is the one-electron reduction of *N*-halogenated species; these processes are stimulated by transition metal ions (Fe^{2+}, Cu^{+}, or Ti^{3+})[12,16,24,25] and $O_2^{\bullet-}$.[26−28] In the case of chloramines and most *N*-brominated species, nitrogen- and carbon-centered radicals and halide ions are generated,[12,16,25,29] but for some *N*-brominated species (e.g., *N*-bromosuccinimide[30,31]) heterolytic cleavage of the N−Br bond may result in the formation of imidyl anions and bromine atoms ($Br^{\bullet}$).

These reactions are of potential importance as both $O_2^{\bullet-}$ and HOCl/HOBr (and hence *N*-halogenated species) are generated concurrently by activated leukocytes, thereby raising the possibility that $O_2^{\bullet-}$ and *N*-halogenated species may interact at inflammatory loci. A key determinant of the importance of these reactions *in vivo* are the relative rate constants for reaction of the *N*-halogenated species with biological targets,[4,11,17,20,32,33] and the rate constants for $O_2^{\bullet-}$ dismutation (reviewed in ref 34). Many of these values have been determined, but the rates of reduction of *N*-halogenated species by $O_2^{\bullet-}$ are unknown. In the current study, the reactions of $O_2^{\bullet-}$ with *N*-halogenated species have been investigated by pulse radiolysis techniques; the *N*-halogenated compounds investigated (Scheme 1) were chosen to model nitrogenous motifs found in biological molecules that are known to react with HOCl/HOBr. The products of one-electron reduction of *N*-brominated species have been probed as these reactions are potentially a novel source of highly damaging bromine atoms *in vivo*. High-level quantum-chemistry calculations have been utilized to provide further insight into the mechanisms of these reactions; these data suggest that the observed processes are general phenomena for *N*-halogenated species.

Scheme 1. Structures of the *N*-Halogenated (X = Cl or Br) Species Investigated in This Study[a]

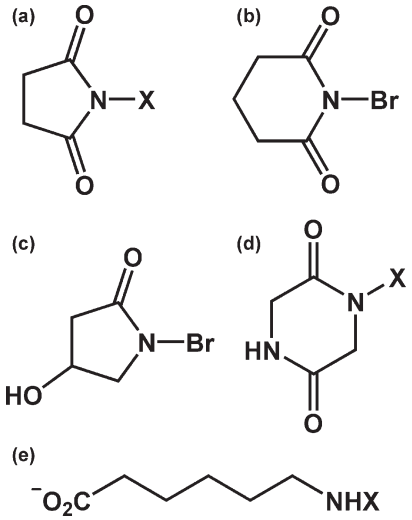

[a] (a) *N*-Chloro- or *N*-bromo-succinimide (NCS or NBS) and (b) *N*-bromoglutarimide (NBG) are models of biological substrates that contain the imide moiety (R-C(O)-NH-C(O)-R′) including some nucleobases and antioxidants. (c) *N*-Bromo-4-hydroxy-2-pyrrolidinone (NBr-HOP) and (d) *N*-bromo or *N*-chloro glycine anhydride ($(Gly)_2Br$ or $(Gly)_2Cl$) were used as models of amide groups, as found primarily in protein backbones. (e) *N*-Chloro- and *N*-bromo-6-amino-caproic acid (CANCl or CANBr) were used to model the chloramines/bromamines formed on the Lys side-chain of proteins, as well as other primary amines.

2. EXPERIMENTAL PROCEDURES

2.1. Materials. Sodium formate and phosphate buffer reagents for pulse radiolysis were obtained from Merck; potassium thiocyanate was from Riedel-de Haen. All other chemicals were obtained from Sigma/Aldrich/Fluka (Castle Hill, NSW, Australia) and used without further purification. HOCl solutions were standardized by measuring the absorbance at 292 nm at pH 12 ($\varepsilon_{292}(^{-}OCl) = 350\ M^{-1}\ cm^{-1}$).[35] All solutions were prepared using water purified by a Millipore "Milli-Q" filtration system, and phosphate buffers utilized for stability studies and extinction coefficient determination were also treated with Chelex resin (BioRad, Hercules, CA, USA) to remove contaminating metal ions.

2.2. Preparation of Hypobromous Acid. HOBr was prepared as described previously[6,14] by mixing HOCl (40 mM) with a 1.125-fold excess of NaBr (45 mM). After 5 min, the resulting HOBr solution was diluted with phosphate buffer to the required concentration.

2.3. Preparation of *N*-Halogenated Species. Concentrated stocks of the *N*-halogenated species were prepared by adding HOCl or HOBr to a solution containing a 2- to 100-fold excess of parent compound in phosphate buffer and were vortexed during and after the addition of HOCl/HOBr to ensure efficient mixing. For kinetic experiments, these concentrated stocks were prepared immediately before use and kept on ice for <1 h; the stock solutions were diluted into the reaction mixture immediately prior to acquisition of the kinetic data. For stability studies and determination of extinction coefficients, the stock solutions were diluted to the desired concentration with phosphate buffer.

2.4. Assay of Concentrations of *N*-Halogenated Species. *N*-Halogenated species were quantified as reported previously[25] using 5-thio-(2-nitrobenzoic acid) (TNB; ca. 40 μM). The extinction coefficient (ε) for TNB at 412 nm was taken as $14150\ M^{-1}\ cm^{-1}$.[36]

2.5. Kinetic Studies. The concentrations of the *N*-halogenated species were determined by measuring their absorbance spectra (Ocean Optics HR 4000 Composite-grating spectrometer) before and after experiments, utilizing published extinction coefficients[37] and those in Table 1. Concentrations of *N*-chlorosuccinimide (NCS) and *N*-bromosuccinimide (NBS) were calculated on a mass basis with subsequent dilution. Reaction mixtures contained 10−500 μM of each substrate in 5 mM phosphate buffer (pH 7.2) solutions.

Time-resolved optical absorption and kinetic studies were carried out at room temperature (22 ± 1 °C) using the University of Auckland's Pulse Radiolysis Facility, which utilizes a 4 MeV linear accelerator to deliver 200 ns electron pulses of 2.5−6 Gy dose to a 2 cm path length cell. The optical detection system and dosimetry method have been reported.[38] The radiolysis of water produces three well-characterized radicals as well as molecular products (eq 1; μM per absorbed dose of 1 Gy (J kg^{-1}) given in parentheses).

$$H_2O \rightsquigarrow e^-_{aq}\ (0.28) + HO^{\bullet}\ (0.28) + H^{\bullet}\ (0.055) + H_2\ (0.04) + H_2O_2\ (0.07) + H_3O^{+}\ (0.28) \quad (1)$$

For experiments designed to study the reactions of $CO_2^{\bullet-}$, solutions containing sodium formate (0.2 M) were presaturated with N_2O gas for 15 min before pulse radiolysis. The addition of formate ions (to scavenge

Table 1. Extinction Coefficients (ε) Determined for the *N*-Brominated Species Utilized in These Studies[a]

substrate	λ (nm)	ε (M^{-1} cm^{-1})
NBG	260	220 ± 10
	280	82 ± 9
$(Gly)_2Br$	260	270 ± 10
	275	162 ± 7
CANBr	290	404 ± 7
NBr-HOP	250	240 ± 20
	280	110 ± 10

[a] All values were calculated from absorbance data at five or six different concentrations, determined in replicate, and repeated on two separate occasions, resulting in $n > 10$ for all values. The errors quoted for each species are presented as 95% confidence intervals. However, for NBr-HOP (250 and 280 nm) and NBG (260 nm), the nonbrominated parent also exhibits a small absorbance at the stated wavelengths resulting in a small systematic error in the reported extinction coefficient.

the $^{\bullet}OH$ radicals and $H^{\bullet}$ atoms) and saturation with N_2O gas (to convert the hydrated electrons (e^-_{aq}) into $^{\bullet}OH$ radicals) results in the exclusive generation of $CO_2^{\bullet-}$ in a yield of 0.68 μM Gy^{-1}.[39] Reactions of $O_2^{\bullet-}$ with the substrates were studied in the same formate-containing solutions which were saturated with O_2 gas, where the e^-_{aq} are scavenged by O_2, and the $CO_2^{\bullet-}$ radical anions undergo fast electron transfer to exclusively form $O_2^{\bullet-}$ (in equilibrium with its protonated form) in the same yield (eqs 2−6).[40] Reactions of the e^-_{aq} species were studied in N_2-saturated solutions containing ^{t}BuOH (0.5 M) to scavenge the $^{\bullet}OH$ radicals and H-atoms (eq 7) to form an inert, nonreducing radical on the alcohol. The reactions of $O_2^{\bullet-}$ were monitored at 260 or 280 nm and those of e^-_{aq} at 620 nm. As $O_2^{\bullet-}$ rapidly dismutates, its stability was also monitored in the absence of any substrates. Bromine atom ($Br^{\bullet}$) formation was monitored by quantifying $Br_2^{\bullet-}$ at 360 nm, through its fast reaction with added bromide ions (1 to 10 mM; eq 8).

$$HO^{\bullet}/H^{\bullet} + HCO_2^- \rightarrow CO_2^{\bullet-} + H_2O/H_2 \quad (2)$$

$$e^-_{aq} + N_2O + H_2O \rightarrow HO^{\bullet} + HO^- + N_2 \quad (3)$$

$$CO_2^{\bullet-} + O_2 \rightarrow O_2^{\bullet-} + CO_2 \quad (4)$$

$$e^-_{aq} + O_2 \rightarrow O_2^{\bullet-} \quad (5)$$

$$HO_2^{\bullet} \rightleftharpoons H^+ + O_2^{\bullet-} \quad (6)$$

$$HO^{\bullet}/H^{\bullet} + (CH_3)_3COH \rightarrow {}^{\bullet}CH_2(CH_3)_2COH + H_2O/H_2 \quad (7)$$

$$Br^{\bullet} + Br^- \rightleftharpoons Br_2^{\bullet-} \quad (8)$$

2.6. Theoretical Procedures. Standard ab initio and density functional theory calculations[41−43] were carried out for a selection of radicals and anions relevant to the one-electron reduction of nitrogen halides using the Gaussian 03 (G03[44]) and Gaussian 09 (G09[45]) programs. Gas-phase structures and harmonic vibrational frequencies were obtained at the B3-LYP/6-31G(2df,p) level. Gas-phase enthalpies and free energies were obtained at the G4 level,[46] including corrections (calculated using appropriately scaled vibrational frequencies[47]) for zero-point vibrational energies, thermal energies, and entropies. These energies allow gas-phase electron affinities and gas-phase free energies for electron addition to be evaluated.

The effect of bulk water was estimated using G03 through the calculation of free energies of solvation (in water) at the HF/6-31+G(d) level in conjunction with the conductor-like polarizable continuum model (CPCM) with Bondi radii.[48,49] This approach provides solvation energies (ΔG_{solv}) with a mean absolute deviation from experimental results of 15.2 kJ mol^{-1} for a test set of 70 species including neutrals, cations, and anions.[50] As the electron-addition reaction does not involve changes in the number of molecules, no change-of-state correction is required to account for the change from the gas phase (1 atm) to solution (1 M). Combination of ΔG(gas) and ΔG_{solv} yields ΔG(aq) values that correspond to 298 K and 1 M H^+. Absolute reduction potentials have then been calculated from ΔG(aq), and finally these are converted to reduction potentials (E^o) relative to the normal hydrogen electrode (NHE). This involves subtracting the estimated absolute reduction potential of 4.43 V for hydrogen[51] from the absolute reduction potentials of the radicals.

2.7. Statistical Analysis. All error bars shown correspond to mean ± 1 SD ($n > 3$ determinations). The errors reported on extinction coefficients and rate constants are 95% confidence limits. However, due to the moderate instability of some of these *N*-halogenated species, these errors indicate the reproducibility of the assays and kinetic determinations, and do not include any systematic errors due to the decomposition of the *N*-halogenated species. All statistical analyses were carried out using Origin Pro 7 (OriginLab Corp.) software.

3. RESULTS

3.1. Stability Studies and Determination of Extinction Coefficients for Relevant *N*-Halogenated Species. The *N*-halogenated species investigated (Scheme 1) were prepared by the addition of HOCl or HOBr (100 μM or 2 mM) to a 2- to 100-fold molar excess of the nonhalogenated parent compounds. *N*-Chlorosuccinimide (NCS) and *N*-bromosuccinimide (NBS) were commercial products. The stabilities of the *N*-brominated species were assessed at 22 °C by directly monitoring their UV/visible spectra (200−320 nm) and/or assaying the concentration of active halogens (HOX or RR′NX species) by the TNB assay,[25] over periods of up to 3 h. Data for related *N*-chlorinated species have been reported.[37]

For *N*-bromo-4-hydroxy-2-pyrrolidinone (NBr-HOP), *N*-bromoglutarimide (NBG), and *N*-bromo glycine anhydride ($(Gly)_2Br$), the UV/visible spectra and stabilities were independent of the molar excess of the nonhalogenated parent. Thus, kinetic studies (see later) were carried out with low molar excesses of substrate over oxidant to minimize interference from the nonhalogenated parents. The yield (relative to the initial HOBr concentration) in each case was ca. 85−90%. NBr-HOP and NBG did not show any decay at room temp over 90 min, whereas $(Gly)_2Br$ decayed to 60− 70% of the initial concentration over this time. As this decay would induce systematic errors into the kinetic data, the stability of $(Gly)_2Br$ was also monitored at 0 °C; under these conditions, minimal decomposition was observed over 3 h.

In contrast, the presence of excess 6-amino-caproic acid, used in the preparation of *N*-bromo-6-amino-caproic acid (CANBr), resulted in significant changes in the UV/visible spectra. This is consistent with equilibration between bromamines and dibromamines,[52] and therefore, CANBr stock solutions were prepared with either a 50- or 100-fold excess of the parent compound over HOBr to minimize dibromamine formation; under these conditions, CANBr accounted for ca. 85% of the HOBr added. The stability of CANBr was not investigated further as the closely related species, *N*-ε-bromo-*N*-α-acetyl-lysine, undergoes minimal decay over 1 h at 37 °C;[28] thus, CANBr is unlikely to

dx.doi.org/10.1021/tx100325z |*Chem. Res. Toxicol.* 2011, 24, 371–382

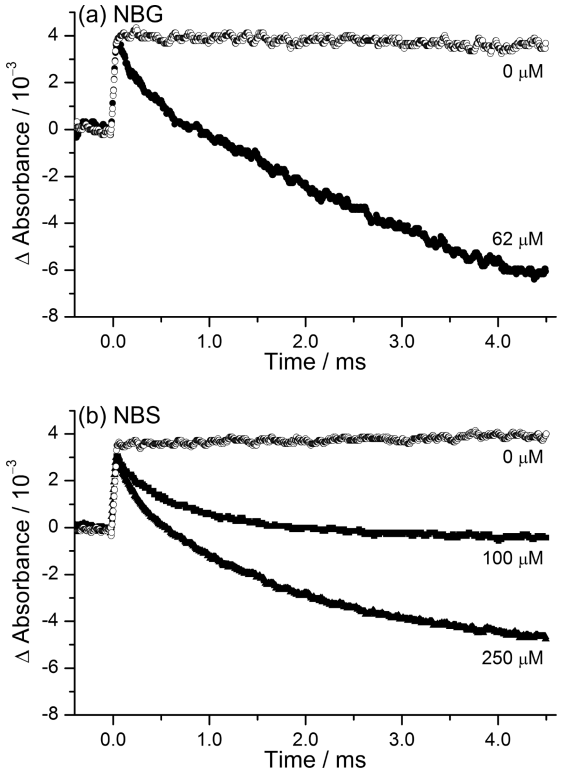

Figure 1. Kinetic traces obtained to follow the reaction of $O_2^{\bullet-}$ (generated in an O_2-saturated solution containing 0.2 M sodium formate and 5 mM phosphate buffer (pH 7.2)) with (a) *N*-bromoglutarimide (0 μM (○) and 62 μM (●)) at 260 nm and (b) *N*-bromosuccinimide (0 μM (○), 100 μM (■), and 250 μM (▲)) at 280 nm. Although these wavelengths were chosen to follow $O_2^{\bullet-}$ consumption, both NBG and NBS also exhibit absorption at these wavelengths, resulting in a significant bleaching of the signals obtained as NBG and NBS are consumed.

decay significantly over 90 min on ice, as confirmed during the kinetic experiments.

The extinction coefficients (ε) for the *N*-brominated species (Table 1) were determined by using multiple dilutions of stock solutions and plotting the observed absorbance (at the wavelength of interest) versus the concentration (as determined by the TNB assay). The derived ε values are consistent with those for other *N*-brominated species[52] and were subsequently used to quantify the stock solutions used in the kinetic studies. ε values for the *N*-chlorinated species have been reported previously.[37]

3.2. Rate Constants for the Reduction of *N*-Halogenated Species by Superoxide. Initial experiments established conditions (0.2 M sodium formate, buffered to pH 7.0−7.2 with 5 mM sodium phosphate, gassed with O_2 for 10−15 min) under which reproducible $O_2^{\bullet-}$ production could be monitored by pulse radiolysis. Under these standard conditions, no decay of the $O_2^{\bullet-}$ signal was observed (at 260 or 280 nm) over time scales up to 5 ms (Figure 1).

3.2.1. N-Bromoglutarimide. Addition of NBG (40−90 μM) to the above system resulted in an enhanced rate of decay of $O_2^{\bullet-}$ (measured at 260 nm; Figure 1a). Biphasic kinetic parameters were required to fit the decays. The observed rate constants derived from the fast component varied from 230 to 5600 s^{-1}, but did not correlate with the NBG concentration present. As a result, a definitive second-order rate constant for the reaction of $O_2^{\bullet-}$ with NBG could not be determined despite clear evidence for a rapid reaction. If it is assumed that the decay at 260 nm monitors only $O_2^{\bullet-}$ and the fast component of the decay is due to the initial reaction of $O_2^{\bullet-}$ with NBG, a lower limit of ca. 3×10^6 M^{-1} s^{-1} can be determined. However, it should be noted that it is not possible mathematically to distinguish which of the decay components corresponds to the $O_2^{\bullet-}$ reaction with NBG. Furthermore, the final absorbance (after 10 ms) of the signal monitored at 260 nm showed extensive bleaching (up to ~0.01 absorbance units; Figure 1a), indicating that detection at 260 nm not only probes the $O_2^{\bullet-}$ concentration but also is influenced by the concentration of NBG (consistent with the extinction coefficient reported in Table 1). The large bleach in signal at 260 nm upon completion of reaction suggests that ca. 23 μM NBG was consumed (using the extinction coefficient in Table 1), which is much greater than the 2−4 μM $O_2^{\bullet-}$ generated during the electron pulse. Further evidence for enhanced NBG loss was obtained when samples were subjected to a second electron pulse without flushing of the sample cell. In this case, no decay of the $O_2^{\bullet-}$ signal at 260 nm was detected, consistent with complete consumption of the NBG following the first electron pulse.

In order to verify that the reduction of NBG was mediated by $O_2^{\bullet-}$ and not its precursor $CO_2^{\bullet-}$ (eqs 1−5), these experiments were repeated under an N_2O atmosphere. Under these conditions, the transient spectrum obtained (with increasing absorbance from 320 nm into the UV region, with a maximum at ca. 250 nm) is consistent with the presence of $CO_2^{\bullet-}$.[53,54] The rate of decay of $CO_2^{\bullet-}$ (at 260 nm) was unchanged by the absence or presence of 50 μM NBG, suggesting that NBG does not react with $CO_2^{\bullet-}$ over these time scales.

3.2.2. N-Bromosuccinimide. The reaction of NBS (100 or 250 μM) with $O_2^{\bullet-}$ was investigated using the standard conditions, but with the signal monitored at 280 nm. At both NBS concentrations, the absorption at 280 nm decayed over a few milliseconds, while in the absence of NBS, no decay was observed over 5 ms (Figure 1b). The decay curves obtained with 100 μM NBS were fitted with a single exponential decay yielding a k_{obs} ca. 1200 s^{-1}, while the data at 250 μM NBS required a double exponential decay to fit accurately, with the observed rate constant for the fast component ranging from 4600 to 8300 s^{-1} and the slower component ca. 500 s^{-1}. These data did not allow a second-order rate constant for NBS + $O_2^{\bullet-}$ to be accurately determined due to the complexity of the decays, but a lower limit of 1×10^7 M^{-1} s^{-1} was determined, on the basis of the fast component of the kinetic decay at 280 nm and the assumption that this monitored only $O_2^{\bullet-}$ consumption. However, as with NBG, a considerable bleaching of the signal was observed at 280 nm consistent with extensive consumption of NBS (indicating chain reactions are occurring), and exposure of the sample to a second electron pulse did not result in decay of the 280 nm signal over 5 ms.

3.2.3. N-Chlorosuccinimide. The reaction of NCS with $O_2^{\bullet-}$ was initially investigated in the standard formate/phosphate solutions. Addition of NCS (100−270 μM) to these solutions resulted in a concentration-dependent increase in the rate of decay of the $O_2^{\bullet-}$ signal at 280 nm. The resulting data were fitted with a single exponential decay, and the first-order rate constants were plotted against the NCS concentration, yielding a second-order rate constant of $(8 \pm 2) \times 10^5$ M^{-1} s^{-1} for the reaction of NCS with $O_2^{\bullet-}$. With higher NCS concentrations (540 μM),

dx.doi.org/10.1021/tx100325z |*Chem. Res. Toxicol.* 2011, 24, 371–382

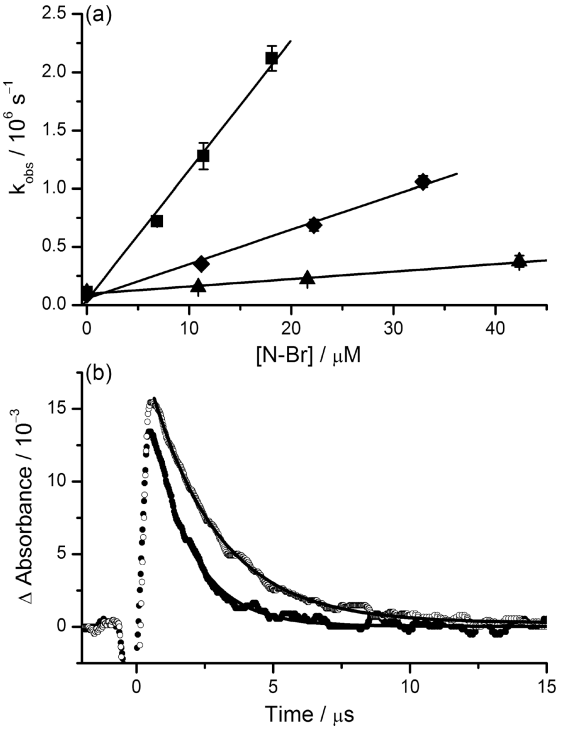

Figure 2. (a) Second-order plots for the quenching of hydrated electrons (monitored at 620 nm) by *N*-bromoglutarimide (■), *N*-bromo-4-hydroxy-2-pyrrolidinone (▲), and *N*-bromo glycine anhydride (♦). The gradients of these linear plots correspond to composite second-order rate constants for the reactions of e^-_{aq} with both the *N*-brominated species and their nonbrominated parents (present in excess; see text). (b) Kinetic traces for the decay of e^-_{aq} (monitored at 620 nm) in the presence of $(Gly)_2$ (190 μM) alone (○) or $(Gly)_2Br$ (22 μM) in the presence of a 10-fold excess of $(Gly)_2$ (●). Single exponential fits to the data are overlaid for both kinetic traces.

interfering reactions of NCS with the primary radiolytically generated radicals resulted in complex kinetics.

3.2.4. Other N-Halogenated Species. The reactions of $O_2^{\bullet-}$ with the other *N*-halogenated species shown in Scheme 1 were also investigated using the standard formate/phosphate solutions. The rate of decay of the $O_2^{\bullet-}$ signal (monitored at 280 nm) was unchanged on addition of CANBr (90 μM), CANCl (265 μM), $(Gly)_2Cl$ (170 μM), or NBr-HOP (60 μM), indicating that $O_2^{\bullet-}$ does not react with these *N*-halogenated species over these time scales.

3.3. Rate Constants for the Reduction of *N*-Halogenated Species by Hydrated Electrons. In the light of the above observations, approximate rate constants for the one-electron reduction of the *N*-brominated species by e^-_{aq} were determined; corresponding data for *N*-chlorinated species have been published.[30,37,55−58]

3.3.1. N-Bromoglutarimide. Reduction of NBG (7−18 μM) by e^-_{aq} was investigated in N_2-saturated solutions containing 0.5 M ^{t}BuOH with 5 mM sodium phosphate buffer (pH 7.2). The loss of e^-_{aq} was monitored at 620 nm over 10−20 μs, and the exponential decays were fitted to yield observed rate constants ranging from 7.2×10^5 s^{-1} to 2.1×10^6 s^{-1} (Figure 2a). The resulting second-order rate constant was calculated as $k_2 = 1.1 \times 10^{11}$ M^{-1} s^{-1} when only the NBG concentration was considered. However, it is not possible for e^-_{aq} to react with such a high rate constant, suggesting that this rate constant is a composite value for the reaction of e^-_{aq} with NBG as well as excess glutarimide (eq 9, where *a* reflects the excess of parent used in preparing the *N*-brominated species).

$$\text{Gradient} = k_2(\text{N} - \text{Br}) + a \times k_2(\text{parent}) \qquad (9)$$

The rate constant for this second process was determined by examining the decay of e^-_{aq} in the presence of glutarimide (200 μM) under identical conditions; this yielded an approximate rate constant of 7×10^9 M^{-1} s^{-1}. These data suggest that the second-order rate constant for the reaction of NBG with e^-_{aq} is $>10^{10}$ M^{-1} s^{-1} (estimated using eq 9 (a = 10)). Unfortunately, accurate determination of this rate constant is not feasible as the rate of decay of e^-_{aq} under these conditions is very fast ($t_{1/2} < 1$ μs), and the reaction with glutarimide is a major contributor to the observed decay, with the pseudo-first-order rate constant for the consumption of e^-_{aq} by glutarimide double that of NBG under these conditions.

A transient spectrum (250−400 nm) obtained 25 μs after e^-_{aq} reduction of NBG (66 μM) displayed a relatively weak absorbance with a maximum at 360 nm. This spectrum did not show any change in features over time, decayed completely by 500 μs, and is consistent with the production of low levels of $Br_2^{\bullet-}$ via bromine atom formation.

3.3.2. $(Gly)_2Br$. The reduction of $(Gly)_2Br$ (11−33 μM) by e^-_{aq} was monitored under conditions identical to those for NBG. As with NBG, the decay of e^-_{aq} is a composite rate of the reactions with $(Gly)_2Br$ and the excess $(Gly)_2$, but the rate of e^-_{aq} decay measured at 620 nm is clearly faster in $(Gly)_2Br$-containing solutions when compared with control solutions containing comparable $(Gly)_2$, but no $(Gly)_2Br$ (Figure 2b). A linear plot of k_{obs} versus [$(Gly)_2Br$] (Figure 2a) yielded a gradient of 3.0×10^{10} M^{-1} s^{-1}. This value corresponds to the sum of the second-order rate constants for $(Gly)_2Br$ and the 10-fold excess of parent $(Gly)_2$. The second-order rate constant for $(Gly)_2$ reacting with e^-_{aq} has been established previously as ca. 1.5×10^9 M^{-1} s^{-1},[37,59] suggesting $k_2 > 1 \times 10^{10}$ M^{-1} s^{-1} (by the use of eq 9 with a = 10) for the reaction of e^-_{aq} with $(Gly)_2Br$. As for NBG, more accurate determination of this rate constant from these data is not appropriate as parent $(Gly)_2$ consumes approximately 50% of the e^-_{aq} under the experimental conditions. However, these data (Figure 2a) suggest that reaction of e^-_{aq} with $(Gly)_2Br$ is slower than that for NBG.

In addition to the kinetics of reaction of $(Gly)_2Br$ with e^-_{aq}, the transient spectra (250−400 nm) were monitored over 1.5 ms with 66 μM $(Gly)_2Br$. At short time scales (ca. 1 μs), a spectrum displaying absorbance maxima at ca. 260 and 360 nm was observed (Figure 3, solid lines). The intensity of this signal reached a maximum after 25 μs, before decaying back to baseline within 1 ms of the initial pulse. The relative intensities of the absorption peaks at 260 and 360 nm remained the same over all time scales, indicating that the spectrum is due to a single species. When the experiments were repeated with parent $(Gly)_2$, this transient spectrum was no longer present, indicating that this intermediate species is formed via the reduction of $(Gly)_2Br$.

3.3.3. NBr-HOP. For the reaction of NBr-HOP (11−42 μM) with e^-_{aq} (Figure 2a), the excess parent HOP was found to react slowly with e^-_{aq}. Thus, the gradient of the linear plot of k_{obs} versus [NBr-HOP] yields the second-order rate constant for e^-_{aq} with NBr-HOP of $k_2 = (6.4 \pm 0.9) \times 10^9$ M^{-1} s^{-1} directly. No further intermediates were detected between 250 and 450 nm over the time scales investigated (up to 9 ms).

3.3.4. CANBr. For the reaction of CANBr with e^-_{aq}, single exponential fitting of the decay traces monitored at 620 nm yielded reproducible k_{obs} values of 1.1×10^6 s^{-1} and 5.7×10^5 s^{-1} at

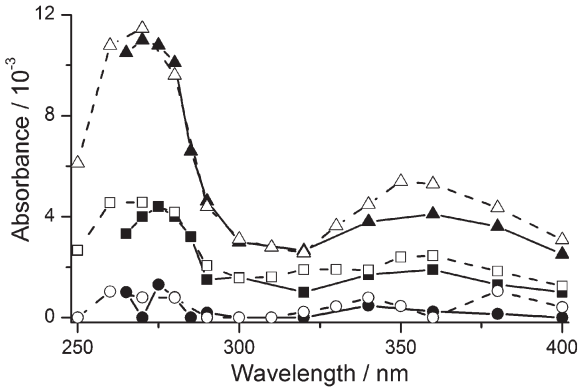

Figure 3. Transient spectra obtained following the reduction of *N*-bromo glycine anhydride by hydrated electrons in the presence (dashed lines, open symbols) or absence (solid lines, solid symbols) of added NaBr (1 mM). The spectra represent those measured immediately after the electron pulse (■,□), after 25 μs (▲,Δ), and 1.5 ms (●,○).

87 μM and 45 μM, respectively. These values yield a second-order rate constant for the reaction of CANBr with e^-_{aq} of ca. 1.2×10^{10} M^{-1} s^{-1}.

3.4. Formation of Bromine Atoms on the Reduction of *N*-Brominated Species. It has been shown experimentally (at pH 9.3)[30] and predicted theoretically[31] that reduction of *N*-bromosuccinimide by e^-_{aq} or $O_2^{\bullet-}$ results in heterolytic cleavage of the N−Br bond to give imidyl anions and free bromine atoms ($Br^\bullet$). Spectra consistent with the formation of low levels of the $Br_2^{\bullet-}$ radical species were also detected during the reduction of NBG by e^-_{aq} in the current studies. In order to confirm the formation of $Br^\bullet$ upon one-electron reduction of the *N*-brominated species in Scheme 1, selected reactions were repeated in the presence of excess Br^- with the potential generation of $Br_2^{\bullet-}$ monitored at 360 nm.[30]

3.4.1. N-Bromosuccinimide. The previous studies[30] on the reduction of NBS by $O_2^{\bullet-}$ to form $Br^\bullet$ were repeated at pH 7.2 to mimic biological pH values, using the standard formate/phosphate solutions supplemented with 1 mM sodium bromide (NaBr). NBS (100 μM) was added to the above solution immediately prior to use to minimize thermal reactions between NBS and Br^-, and the formation of $Br_2^{\bullet-}$ was monitored at 360 nm. In the absence of added Br^-, a small exponential growth was observed over 200 μs (k, 1.3×10^4 s^{-1}), probably due to the presence of low concentrations of Br^- in NBS. Addition of 1 mM NaBr enhanced the signal intensity ca. 10-fold, with the growth phase having k, 2×10^4 s^{-1} (Figure 4a). These signals decayed to baseline over 5 ms (Figure 4b) with an observed first-order rate constant of ca. 10^3 s^{-1}; these decay rates are of the same order as those obtained for $Br_2^{\bullet-}$ produced in an N_2O-saturated solution containing 5 mM phosphate buffer (pH 7.2) and 1 mM NaBr (data not shown).

The above experiments were repeated in ^{t}BuOH/phosphate solutions to investigate the reactions of NBS (100 μM) with e^-_{aq}. The traces obtained at 360 nm in the presence of 1 mM NaBr displayed an enhancement in signal intensity (as seen with $O_2^{\bullet-}$), confirming that e^-_{aq}-mediated reduction of NBS also results in a signal consistent with the formation of $Br^\bullet$. The first-order rate constant for the growth of $Br_2^{\bullet-}$ under these conditions was considerably faster than that with the $O_2^{\bullet-}$ system ($(7 \pm 1) \times 10^4$ s^{-1}), while the subsequent decay could not be fitted accurately with a single exponential function.

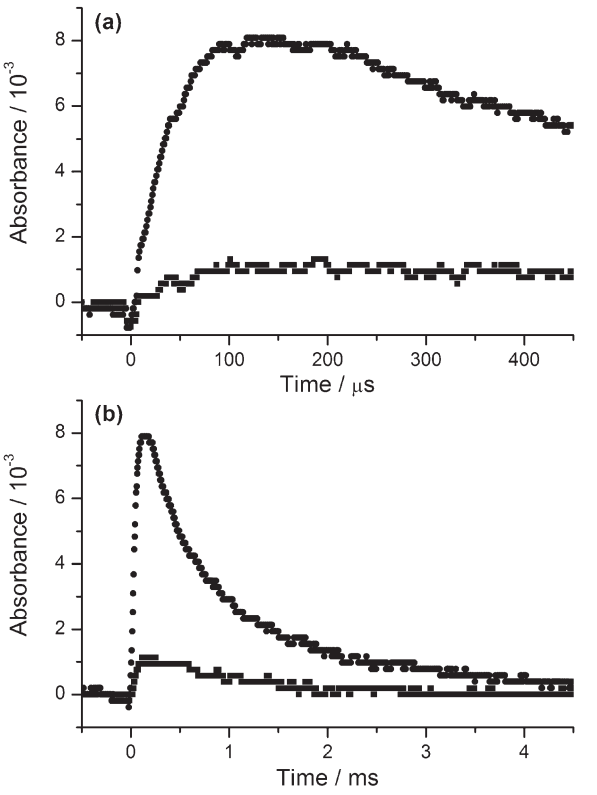

Figure 4. Kinetic traces (360 nm) obtained following the reaction of *N*-bromosuccinimide (100 μM) with $O_2^{\bullet-}$ (generated in an O_2-saturated solution containing 0.2 M sodium formate and 5 mM phosphate buffer (pH 7.2)) in the absence (■) and presence (●) of 1 mM NaBr. Panel a shows the growth of the signal attributed to $Br_2^{\bullet-}$ over 200 μs, with b showing the subsequent decay of this signal over 5 ms.

3.4.2. N-Bromoglutarimide. The formation of $Br^\bullet$ following one-electron reduction of NBG (66 μM) by e^-_{aq} was probed (at 360 nm) in the presence or absence of added 1 mM NaBr. In the presence of added NaBr, the signal was approximately 3-fold greater in intensity, with a rate of growth ($k_{obs} \sim 6 \times 10^4$ s^{-1}) very similar to that in the absence of NaBr, providing good evidence for the formation of $Br_2^{\bullet-}$ and, by inference, $Br^\bullet$. This signal subsequently decayed over a period of ca. 3 ms with unresolved mixed-order kinetics.

3.4.3. Other N-Brominated Species. The reactions of $(Gly)_2Br$ (48 μM) and CANBr (87 μM) with e^-_{aq} were examined in a similar manner; in both cases, there was no significant signal enhancement at 360 nm. In agreement with this observation, the transient spectra (250−400 nm) obtained following the reduction of $(Gly)_2Br$ in the presence of 1 mM (Figure 3, solid lines and symbols) or 10 mM NaBr demonstrated only a minor increase in absorbance at 360 nm compared with the absence of NaBr. These data suggest that $Br^\bullet$ is not generated on reduction of $(Gly)_2Br$ or CANBr.

3.5. Theoretical Investigations. High-level quantum chemistry computations have been undertaken to help rationalize the experimental observations. Initially, the gas-phase electron affinities (EA) were calculated for a selection of species relevant to the one-electron reduction of *N*-halogenated species. The EA is defined as the energy liberated when an electron is added to a neutral species (i.e., the negative of the energy change for the reaction shown in eq 10). A positive EA thus corresponds to a situation in which the electron is bound to the neutral species $X^\bullet$.

Table 2. Calculated Gas-Phase Electron Affinities (EA), Radical Stabilization Energies (RSE), and Anion Stabilization Energies (ASE) (G4, 298 K, kJ mol^{-1}), Aqueous Free Energies of Solvation ($\Delta\Delta G_{solv}$, HF/6-31+G(d), kJ mol^{-1}), and Reduction Potentials (E^o, V)[a]

species	EA	RSE	ASE	$\Delta\Delta G_{solv}$[h]	E^o
$NH_2^\bullet$	74.3 (74.4)[b]	0.0	0.0	−360.5	0.06
$CH_3NH^\bullet$	43.6 (41.7)[c]	32.2	1.5	−326.1	−0.63
$CF_3NH^\bullet$	263.4	−5.4	183.7	−260.0	0.97
imidazolyl$^\bullet$	252.9 (252.1)[d]	47.0	225.6	−238.4	0.64
$HCONH^\bullet$	279.8	−26.9	178.6	−278.0	1.24
$(CHO)_2N^\bullet$	383.4	−43.9	265.2	−225.2	1.90
succinimidyl$^\bullet$	384.8[e]	−56.9[e]	253.6	−241.4	1.97 (2.22)[i]
$Br^\bullet$	327.5 (324.5)[f]			−276.9	1.82 (1.92)[i]
$Cl^\bullet$	345.7 (348.7)[g]			−309.3	2.34 (2.41)[i]

[a] Experimental values are in parentheses. [b] Experimental value from ref 61. [c] Experimental value from ref 60. [d] Experimental value from ref 63. [e] The gas-phase electron affinity and radical stabilization energy of the succinimidyl radical are based on the cyclic ($^2A'$) structure rather than the lower energy acyclic carbon-centered β-(isothiocyanatocarbonyl)ethyl radical. [f] Experimental value from ref 64. [g] Experimental value from ref 65. [h] Defined as the difference between ΔG_{solv} (X^-) and ΔG_{solv} ($X^\bullet$). [i] Experimental values from ref 55.

The systems investigated provide representative examples of the species investigated experimentally. Thus, the EAs have been calculated (Table 2) for *N*-centered radicals derived from the halogenated derivatives of two amines ($CH_3NH^\bullet$ and $CF_3NH^\bullet$), an amide ($HCONH^\bullet$), two imides (succinimidyl radical and $(CHO)_2N^\bullet$), and chlorine and bromine atoms. Good agreement was observed between the calculated (G4) and available experimental[60−65] gas-phase EAs (Table 2), with the differences between theory and experiment all less than 5 kJ mol^{-1}.

$$X^\bullet + e^- \rightarrow X^- \quad (10)$$

In order to facilitate analysis of the calculated EAs for the various *N*-centered radicals (Table 2), it is convenient to define the radical stabilization energy (RSE) of these species as the energy change for the formal reaction presented in eq 11. The RSE measures the effect of the substituent X on the stability of the radical $XNH^\bullet$ relative to its effect in the closed-shell molecule XNH_2. A positive value indicates relative stabilization of the radical. Similarly, the anion stabilization energy (ASE) is defined as the energy change for the formal reaction shown in eq 12. The ASE measures the effect of the substituent X on the stability of the anion XNH^- relative to its effect in the neutral XNH_2. A positive value indicates relative stabilization of the anion. Finally, the effect of the substituent X on the EA of the radical $XNH^\bullet$ [$\Delta EA(XNH^\bullet) = EA(XNH^\bullet) - EA(NH_2^\bullet)$] is related simply to the RSE($(XNH^\bullet)$ and ASE(XNH^-) values (eq 13).

$$XNH^\bullet + NH_3 \rightarrow XNH_2 + NH_2^\bullet \quad (11)$$

$$XNH^- + NH_3 \rightarrow XNH_2 + NH_2^- \quad (12)$$

$$\Delta EA(XNH^\bullet) = ASE(XNH^-) - RSE(XNH^\bullet) \quad (13)$$

These calculations show that a methyl substituent has a considerably greater stabilizing effect in $CH_3NH^\bullet$ (RSE = 32.2 kJ mol^{-1}) than in CH_3NH^- (ASE = 1.5 kJ mol^{-1}). This leads to the EA of $CH_3NH^\bullet$ actually being *lower* (by 30.7 kJ mol^{-1}) than that of the parent compound $NH_2^\bullet$. However, substitution of one of the hydrogen atoms of $NH_2^\bullet$ with the electron-withdrawing CF_3 substituent leads to an increase in the EA of the resulting radical ($CF_3NH^\bullet$) by 189.1 kJ mol^{-1} compared with $NH_2^\bullet$. This significant increase in EA can be partially attributed to a relative destabilizing effect in the radical (RSE = −5.4 kJ mol^{-1}, consistent with previous investigations e.g., ref 66 and references therein), but is predominantly due to the large stabilizing effect in the anion (ASE = 183.7 kJ mol^{-1}).

Analogously, substitution with a single (electron-withdrawing) formyl substituent, as in the case of $HCONH^\bullet$, leads to a much higher EA (279.8 kJ mol^{-1}). This increase can likewise be attributed to the existence of a small destabilizing effect of −26.9 kJ mol^{-1} in the radical (consistent with previous data[66]) but a substantial stabilizing effect (of 178.6 kJ mol^{-1}) in the anion. A second formyl substituent, as exists in the $(CHO)_2N^\bullet$ radical, leads to further destabilization of the radical (RSE = −43.9 kJ mol^{-1}) and further stabilization of the anion (ASE = 265.2 kJ mol^{-1}), although the effect of the second substituent is smaller than that of the first. The combined effect of destabilization of the radical and substantial stabilization of the anion leads to the high EA of the $(CHO)_2N^\bullet$ radical (383.4 kJ mol^{-1}). Similar contributions lead to the high EA of the succinimidyl radical (384.8 kJ mol^{-1}).

The gas-phase EAs (Table 2) of both $Cl^\bullet$ (345.7 kJ mol^{-1}) and $Br^\bullet$ (327.5 kJ mol^{-1}) are lower than those of the $(CHO)_2N^\bullet$ radical (383.4 kJ mol^{-1}) and the succinimidyl radicals (384.8 kJ mol^{-1}). This indicates that in the gas-phase, one-electron reduction of both the *N*-chloro and *N*-bromo derivatives of these imides should give rise to $Cl^\bullet/Br^\bullet$ and the imidyl anions rather than Cl^-/Br^- and the imidyl radicals.

In order to allow a more meaningful comparison of the calculated results with experiments in aqueous solution, the influence of aqueous solvation on the thermodynamics of one-electron reduction was investigated. The calculations for $\Delta\Delta G_{solv} = \Delta G_{solv}(X^-) - \Delta G_{solv}(X^\bullet)$ (Table 2) yield large negative values, reflecting the considerably greater solvation of anions compared with that of neutral radicals. The calculated reduction potentials (E °) are given in Table 2.

The solvation energies are very sensitive to the model employed for the small *N*-centered anions, and the calculated E^o values consequently have considerably greater associated uncertainty than the underlying gas-phase EAs. As a result, the agreement between calculated and experimental[55,67] reduction potentials is typically poorer. The solvation energies vary quite widely for the different species, dependent in part on molecular size. For example, the solvation energy for the smaller Cl^- (−309.3 kJ mol^{-1}) is considerably larger than that for the bulkier succinimidyl anion (−241.4 kJ mol^{-1}).

As a result of the differential solvation effects, in water the succinimidyl radical no longer gives rise to the most favorable one-electron reduction. The calculated E^o (1.97 V) is less than that for $Cl^\bullet$ (E^o = 2.34 V), which therefore undergoes preferential one-electron reduction in solution. Br^- also has a greater solvation energy than the succinimidyl anion, but in this case, it is not sufficient to override the gas-phase ranking of EAs, with the one-electron reduction (E^o = 1.82 V) slightly less favorable than that for the succinimidyl radical (E^o = 1.97 V). The calculated E^o for the acyclic $(CHO)_2N^\bullet$ radical is also greater than that of $Br^\bullet$ (1.90 V vs 1.82 V) indicating that the imidyl radical, and not $Br^\bullet$, would undergo preferential reduction.

dx.doi.org/10.1021/tx100325z |*Chem. Res. Toxicol.* 2011, 24, 371–382

Once a theoretical basis for the experimental observations was established, it was investigated whether a correlation exists between the rates of one-electron reduction of *N*-halogenated species and the thermodynamics of their reduction. Using the reduction of MeNHCl and MeNHBr as probes (eq 14), (gas-phase) enthalpies were calculated for these processes. These calculations suggest that the reduction of MeNHCl is associated with a reduced exothermicity (99.5 kJ mol^{-1}) compared with that of MeNHBr (122.1 kJ mol^{-1}). This ordering parallels the faster observed reduction rates for the *N*-bromo species and suggests that the relative strengths of N−X bonds is an important factor governing the reduction rates.

$$MeNHX + e^- \rightarrow MeNH^\bullet + X^- \quad (14)$$

4. DISCUSSION

4.1. Absolute Rate Constants for e^-_{aq}-Mediated Reduction of *N*-Halogenated Species. It is well established that one-electron reduction of *N*-halogenated species results in the heterolytic cleavage of the N−X bond to yield an anion and a radical species. Rate constants for the reduction of *N*-chlorinated species by e^-_{aq} are close to diffusion-controlled ($k_2 \geq 10^9$ M^{-1} s^{-1}).[37,55−58,68] The fastest reactions are for the *N*-chloroimides, with rate constants (k_2) for *N*-chloroglutarimide and *N*-chlorosuccinimide of 1.9×10^{10} M^{-1} s^{-1} and 1.6×10^{10} M^{-1} s^{-1}, respectively.[55,68] Similar high values (ca. 1.5×10^{10} M^{-1} s^{-1}) have been reported for the *N*-chloroamides of the cyclic dipeptides of $(Gly)_2$ and $(Ala)_2$.[37] Reduction of monochloramine (NH_2Cl) by e^-_{aq} occurs with a similar rate constant (k_2, 2.2×10^{10} M^{-1} s^{-1} [56,57]), while the rate constants for the e^-_{aq}-mediated reduction of *N*-chlorinated primary amines (RNHCl) vary from $6.1-9.3 \times 10^9$ M^{-1} s^{-1} (e.g., (k_2(CA-NCl + e^-_{aq}), 9.3×10^9 M^{-1} s^{-1}).[37] The *N*-chlorinated species with the lowest measured rate constant with e^-_{aq} is (*N*-chloro, *N*-phenyl)glycine with $k_2 = 2.9 \times 10^9$ M^{-1} s^{-1};[58] this lower reactivity is presumably due to perturbation of the electron density at the nitrogen center by the phenyl ring.

In contrast to these *N*-chlorinated species, few data are available for *N*-brominated compounds with e^-_{aq}, with the only reported rate constant that we are aware of being for *N*-bromosuccinimide with $k_2 = 2.9 \times 10^{10}$ M^{-1} s^{-1}.[30] This rate constant is 1.8 times faster than the corresponding reaction for NCS. Thus, the approximate rate constants (>10^{10} M^{-1} s^{-1}) determined here for *N*-bromoglutarimide, $(Gly)_2Br$, and CANBr compare favorably with those expected on the basis of the corresponding *N*-chloro data. Typically, a small increase in rate constant is observed for the *N*-bromo compared with the *N*-chloro species; this may, in part, be attributed to the relative weakness of N−Br compared with N−Cl bonds (see above).

4.2. Species Generated by Reduction of *N*-Halogenated Imides. In all cases, reduction of the *N*-chlorinated species has been attributed to the cleavage of the N−Cl bond to yield the corresponding *N*-centered radical and Cl^-. This process is believed to occur via the formation of a radical anion intermediate. This species has been observed in the case of $NCS^{\bullet-}$,[55] but not with other *N*-chlorinated species.[37,56−58] The rate constant for the decomposition of $NCS^{\bullet-}$ to the succinimidyl radical and chloride has previously been determined as 8×10^5 s^{-1},[55] similar to that found here ($\sim 7 \times 10^5$ s^{-1}). In contrast to $NCS^{\bullet-}$, which has a moderate lifetime at room temperature,[55] $NBS^{\bullet-}$ has only been detected at 77 K by EPR spectroscopy.[30] This observation is consistent with the current results where no intermediates (other than $Br_2^{\bullet-}$) were observed for NBS or NBG.

In the current studies, the formation of $Br^\bullet$ on reduction of NBS or NBG by $O_2^{\bullet-}$ or e^-_{aq} was demonstrated by the enhancement of a transient signal at 360 nm in the presence of 1 mM Br^-, consistent with the formation of $Br_2^{\bullet-}$. The detection of low yields of $Br_2^{\bullet-}$ in the absence of added Br^- is believed to be due to low levels of Br^-/Br_2 in the commercial NBS, and the preparation of NBG from Br^--containing HOBr. For both NBS and NBG, the $Br_2^{\bullet-}$ signal displayed a small rapid rise, followed by a growth phase with first-order rate constants of 10^4-10^5 s^{-1}. Lind et al. utilized the observed rate of formation of $Br_2^{\bullet-}$ to derive the second-order rate constant for the reaction of $O_2^{\bullet-}$ with NBS (k_2, 5×10^8 M^{-1} s^{-1}), with the assumption that the rate-determining step in this reaction was the reduction of NBS at Br^- concentrations >1 mM.[30] With the current data, this approach yields an approximate second-order rate constant of 2×10^8 M^{-1} s^{-1} for the reaction of NBS with $O_2^{\bullet-}$ consistent with previous reports.[30] This value is considerably larger than the lower limit derived above from the consumption of $O_2^{\bullet-}$ at 260 nm, and provides a more robust estimate of this rate constant given that it is mathematically impossible to distinguish, from a single data set, which of two consecutive reactions are faster. A similar approach can be employed to analyze the e^-_{aq}-mediated reduction of NBS and NBG, yielding second-order rate constants of 6.7×10^8 and 9×10^8 M^{-1} s^{-1} respectively, which are markedly lower than those obtained (>10^{10} M^{-1} $s^{-1}$from ref 30 and this work) from direct quenching of e^-_{aq} (>600 nm). It is possible that this discrepancy arises from $NBS^{\bullet-}$ and $NBG^{\bullet-}$ having lifetimes that are measurable on the time scale of pulse radiolysis, similar to that reported by Lind et al. for the reduction of *N*-bromophthalimide (PBr) to form $PBr^{\bullet-}$ (λ_{max}, 325 nm) which decomposes relatively slowly ($k < 10^5$ s^{-1}) to form $Br^\bullet$.[30] However, the reported lifetime of $NBS^{\bullet-}$ is too short to measure on the pulse radiolysis time scale.[30] Thus, it is more likely that the relatively slow rates of growth of $Br_2^{\bullet-}$ arise from chain reactions that release $Br^\bullet$ as one of the radical chain carriers.

4.3. Initiation of Chain Reactions Following the Reduction of *N*-Brominated Imides. Complex chain reactions have been identified in synthetic bromination reactions mediated by NBS, though the identities of the chain carriers has been a source of debate.[69,70] Pulse radiolysis studies on one-electron reduction of NBS[30,55,68,71] have demonstrated that multiple radicals can be involved, including competing chains involving succinimidyl radicals ($S^\bullet$) and $Br^\bullet$.[30,71] The current data for $O_2^{\bullet-}$-mediated reduction of NBS and NBG are consistent with such processes, as the extent of NBS/NBG loss (estimated from the bleaching of the signal at 260 or 280 nm) is ca. 10 to 20 times the amount of $O_2^{\bullet-}$ generated by the electron pulse. The occurrence of chain reactions in the e^-_{aq}-mediated reduction of NBS and NBG is not apparent in the current studies, as the reaction was not monitored below 300 nm where NBS/NBG absorb. However, the slow production of the $Br_2^{\bullet-}$ signal (360 nm; reaction 8) compared with the consumption of e^-_{aq} (620 nm) is consistent with secondary $Br^\bullet$ formation (eqs 15 and 16) during chain reactions, as described previously.[71]

$$^\bullet CH_2(CH_3)_2COH + Br_2 \rightarrow BrCH_2(CH_3)_2COH + Br^\bullet \quad (15)$$

$$S^\bullet + Br^- \rightarrow S^- + Br^\bullet \quad (16)$$

dx.doi.org/10.1021/tx100325z |*Chem. Res. Toxicol.* 2011, 24, 371–382

Scheme 2. Proposed Reaction Mechanism for the Reduction of *N*-Bromo Glycine Anhydride ($(Gly)_2Br$) by Hydrated Electrons (e^-_{aq}), with Initial Formation of an Amidyl Radical and a Subsequent Rapid 1,2-Shift to Yield an α-Carbon-Centered Radical

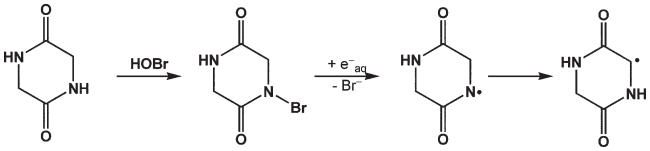

4.4. Radicals Generated by the Reduction of the *N*-Bromamide, $(Gly)_2Br$. In contrast to the complex behavior observed with the *N*-bromo imides, e^-_{aq} reduction of $(Gly)_2Br$ resulted in a transient with absorption maxima at 260 and 360 nm (Figure 3). A similar transient has been reported for the reaction of $HO^\bullet$ with $(Gly)_2$,[59] but control experiments with $(Gly)_2$ alone confirmed that this reaction is not the source of this intermediate. The observed absorption is different from that arising from the reaction of $(Gly)_2$ with e^-_{aq}, with this yielding a spectrum with a single absorption maximum that rises into the UV region (λ_{max} < 240 nm).[59] Thus, it is proposed that the reaction of $(Gly)_2Br$ with e^-_{aq} cleaves the N−Br bond to form an *N*-centered radical and Br^- (rather than $Br^\bullet$). The resulting *N*-centered radical undergoes a rapid 1,2-shift to yield the same carbon-centered radical generated on reaction of $HO^\bullet$ with $(Gly)_2$ (Scheme 2). This mechanism is well established for *N*-chlorinated *N*-acetyl amino acids,[16,24] and the corresponding radical has been detected by EPR spin-trapping studies of $(Gly)_2Br$.[29]

4.5. Theoretical Investigations. The calculated reduction potentials in aqueous solution (Table 2) are consistent with the experimental findings. In the first place, the present calculations confirm that one-electron reduction of *N*-chloro- or *N*-bromo-amides or -amines should give rise to *N*-centered radicals plus Cl^-/Br^- rather than *N*-centered anions plus $Cl^\bullet/Br^\bullet$ because the halides are better able than the amido or amino moieties to accommodate the negative charge. In contrast, one-electron reduction of *N*-bromosuccinimide should yield $Br^\bullet$ plus succinimidyl anion, but this preference is small. Finally, the one-electron reduction of the N−Cl bond of *N*-chlorosuccinimide is predicted to yield the succinimidyl radical and Cl^- preferentially because of the larger E^o for $Cl^\bullet$ than for the succinimidyl radical.

Comparison of the calculated reduction potentials for the radicals of interest with the experimentally derived value for the $O_{2(aq)}/O_2^{\bullet-}{}_{(aq)}$ couple (reevaluated recently as −0.18 V[72]) established that reduction by $O_2^{\bullet-}$ is thermodynamically favorable for all of the radicals investigated, except $MeNH^-$ and possibly NH_2^-. This is an important conclusion as it resolves the apparent paradox that only *N*-halogenated imides are reduced by $O_2^{\bullet-}$ on the pulse radiolysis time scale, whereas steady state studies show that $O_2^{\bullet-}$ does reduce the other *N*-halogenated species.[26−28]

4.6. Conclusions. The current kinetic studies have shown that *N*-halogenated species readily undergo one-electron reduction. In the case of the *N*-chlorinated species, and many of the *N*-brominated species, one-electron reduction by e^-_{aq} or $O_2^{\bullet-}$ results in the production of *N*-centered radicals.[16,24,29,68] However, in *N*-bromoimides the favored reduction pathway leads to the production of $Br^\bullet$, which can initiate radical chain reactions of moderate length (ca. 10−20). These observations are consistent with E^o values obtained from high-level quantum chemical computations. Furthermore, preliminary calculations (O'Reilly et al., unpublished data) on more biologically relevant imide-containing substrates indicate, for example, that one-electron reduction of *N*-bromouracil would be expected to generate $Br^\bullet$ and the nitrogen-centered uracil anion, whereas the reverse is true for *N*-chlorouracil.

These reactions of *N*-halogenated imides may be of biological importance as it is well established, for example, that the levels of 5-bromo- and 5-chloro-uracil are markedly elevated in inflammatory tissue and atherosclerotic lesions in humans.[73,74] In addition, levels of parent uracil are massively elevated in human inflammatory tissue (up to 600 μM, ca. 1000-fold higher than plasma concentrations[73]). The mechanism of formation of the modified bases is unclear, but may well involve *N*-chlorinated or *N*-brominated intermediates (reviewed in ref 4). In addition to uracil, these imide moieties are present in thymine and purine metabolites such as xanthine and urate (plasma concentrations are ∼5 μM and 200−300 μM, respectively [75]), all of which react readily with HOCl,[11] and should react readily with HOBr (reviewed in ref 4). These observations suggest that the *in vivo* formation of *N*-brominated and *N*-chlorinated imide species is likely to occur at sites of inflammation, particularly within the phagosomes of activated white cells that phagocytose foreign organisms and apoptotic cells.

It is known that $O_2^{\bullet-}$ and H_2O_2 are also generated in phagosomes by NOX enzymes as part of the inflammatory response.[1] While concentrations of $O_2^{\bullet-}$ are typically considered to be quite low (submicromolar), modeling studies suggest that in the small volume of the phagosome, $O_2^{\bullet-}$ is generated at a flux of 5.2 mM s^{-1} and reaches a steady state concentration of 25 μM.[76] Thus, while the current kinetic studies cannot provide definitive rate constants for the interaction of $O_2^{\bullet-}$ with *N*-halogenated imides due to the initiation of chain reactions, these reactions are clearly favorable with relatively fast rate constants (>10^6 M^{-1} s^{-1}). These data suggest that the production of activated *N*-halogenated species in the presence of elevated phagosomal $O_2^{\bullet-}$ concentrations might induce tissue damage *in vivo* through the formation of destructive organic radicals and $Br^\bullet$, especially as these species can elicit efficient chain reactions.

■ ASSOCIATED CONTENT

Supporting Information. Gaussian archive entries for B3-LYP/6-31G(2df,p) optimized geometries for all structures investigated (Table S1) and G4 electronic energies, vibrational corrections, free energies of solvation, and G4 free energies (Table S2). This material is available free of charge via the Internet at http://pubs.acs.org.

■ AUTHOR INFORMATION

Corresponding Author

*Tel: +61-2-8208-8900. Fax: +61-2-9565-5584. E-mail: pattisond@hri.org.au.

Funding Sources

This work was supported by grants from AINSE Ltd (Award No. AINGRA07035), the Australian Research Council (ARC Centres of Excellence grant CE0561607, and Discovery program

grants DP0988311 and DP1095821), and the National Heart Foundation (Grants in Aid: G09S4313 and G08S3769).

■ ACKNOWLEDGMENT

We thank Drs. Sujata Shinde and Andrej Maros, and Mr. Grant Woodroffe for technical expertise at the Auckland Pulse Radiolysis Facility, and Drs. Clare Hawkins and Martin Rees for invaluable discussions. The generous allocations of computing time from the National Computational Infrastructure (NCI) National Facility and from Intersect Australia Ltd. are also gratefully acknowledged.

■ ABBREVIATIONS

ASE, anion stabilization energy; $Br^{\bullet}$, bromine atoms; ^{t}BuOH, *tert*-butanol; CANBr, *N*-bromo-6-amino-caproic acid; CANCl, *N*-chloro-6-amino-caproic acid; $Cl^{\bullet}$, chlorine atoms; CPCM, conductor-like polarizable continuum model; DTNB, 5,5′-dithiobis-(2-nitrobenzoic acid); e^{-}_{aq}, hydrated electron; E^{o}, reduction potential; EA, electron affinity; EPO, eosinophil peroxidase; $(Gly)_2$, cyclic Gly dipeptide (also known as glycine anhydride); G03, Gaussian 03 program; G09, Gaussian 09 program; G4, Gaussian 4 theory; $(Gly)_2Br$, *N*-bromo glycine anhydride; $(Gly)_2Cl$, *N*-chloro glycine anhydride; HOBr, the equilibrium mixture of hypobromous acid and its anion, OBr^{-}, at physiological pH 7.4; HOCl, the equilibrium mixture of hypochlorous acid and its anion, OCl^{-}, at physiological pH 7.4; MPO, myeloperoxidase; NBG, *N*-bromoglutarimide; NBr-HOP, *N*-bromo-4-hydroxy-2-pyrrolidinone; NBS, *N*-bromosuccinimide; NCS, *N*-chlorosuccinimide; NHE, normal hydrogen electrode; RSE, radical stabilization energy; TNB, 5-thio-2-nitrobenzoic acid.

■ REFERENCES

(1) Babior, B. M. (2004) NADPH oxidase. *Curr. Opin. Immunol. 16*, 42–47.

(2) Davies, M. J., Hawkins, C. L., Pattison, D. I., and Rees, M. D. (2008) Mammalian heme peroxidases: From molecular mechanisms to health implications. *Antioxid. Redox Signaling 10*, 1199–1234.

(3) Klebanoff, S. J. (2005) Myeloperoxidase: friend and foe. *J. Leukocyte Biol. 77*, 598–625.

(4) Pattison, D. I., and Davies, M. J. (2006) Reactions of myeloperoxidase-derived oxidants with biological substrates: Gaining chemical insight into human inflammatory diseases. *Curr. Med. Chem. 13*, 3271–3290.

(5) Pattison, D. I., and Davies, M. J. (2001) Absolute rate constants for the reaction of hypochlorous acid with protein side-chains and peptide bonds. *Chem. Res. Toxicol. 14*, 1453–1464.

(6) Pattison, D. I., and Davies, M. J. (2004) A kinetic analysis of the reactions of hypobromous acid with protein components: implications for cellular damage and the use of 3-bromotyrosine as a marker of oxidative stress. *Biochemistry 43*, 4799–4809.

(7) Winterbourn, C. C. (1985) Comparative reactivities of various biological compounds with myeloperoxidase-hydrogen peroxide-chloride, and similarity of the oxidant to hypochlorite. *Biochim. Biophys. Acta 840*, 204–210.

(8) Hawkins, C. L. (2009) The role of hypothiocyanous acid (HOSCN) in biological systems. *Free Radical Res. 43*, 1147–1158.

(9) Nagy, P., Jameson, G. N., and Winterbourn, C. C. (2009) Kinetics and mechanisms of the reaction of hypothiocyanous acid with 5-thio-2-nitrobenzoic acid and reduced glutathione. *Chem. Res. Toxicol. 22*, 1833–1840.

(10) Skaff, O., Pattison, D. I., and Davies, M. J. (2009) Hypothiocyanous acid reactivity with low-molecular-mass and protein thiols: absolute rate constants and assessment of biological relevance. *Biochem. J. 422*, 111–117.

(11) Prutz, W. A. (1998) Interactions of hypochlorous acid with pyrimidine nucleotides, and secondary reactions of chlorinated pyrimidines with GSH, NADH, and other substrates. *Arch. Biochem. Biophys. 349*, 183–191.

(12) Rees, M. D., Hawkins, C. L., and Davies, M. J. (2003) Hypochlorite-mediated fragmentation of hyaluronan, chondritin sulfates, and related *N*-acetyl glycosamines: Evidence for chloramide formation, free radical transfer reactions and site-specific fragmentation. *J. Am. Chem. Soc. 125*, 13719–13733.

(13) Pattison, D. I., Hawkins, C. L., and Davies, M. J. (2003) Hypochlorous acid mediated oxidation of lipid components present in low-density lipoproteins: absolute rate constants, product analysis and computational modeling. *Chem. Res. Toxicol. 16*, 439–449.

(14) Skaff, O., Pattison, D. I., and Davies, M. J. (2007) Kinetics of hypobromous acid-mediated oxidation of lipid components and antioxidants. *Chem. Res. Toxicol. 20*, 1980–1988.

(15) Spickett, C. M. (2007) Chlorinated lipids and fatty acids: an emerging role in pathology. *Pharmacol. Ther. 115*, 400–409.

(16) Hawkins, C. L., and Davies, M. J. (1998) Reaction of HOCl with amino acids and peptides: EPR evidence for rapid rearrangement and fragmentation reactions of nitrogen-centered radicals. *J. Chem. Soc., Perkin Trans. 2*, 1937–1945.

(17) Pattison, D. I., Hawkins, C. L., and Davies, M. J. (2007) Hypochlorous acid-mediated protein oxidation: How important are chloramine transfer reactions and protein tertiary structure?. *Biochemistry 46*, 9853–9864.

(18) Hazen, S. L., d'Avignon, A., Anderson, M. A., Hsu, F. F., and Heinecke, J. W. (1998) Human neutrophils employ the myeloperoxidase-hydrogen peroxide-chloride system to oxidise α-amino-acids to a family of reactive aldehydes. *J. Biol. Chem. 273*, 4997–5005.

(19) Armesto, X. L., Canle, M. L., Garcia, M. V., and Santaballa, J. A. (1998) Aqueous chemistry of *N*-halo-compounds. *Chem. Soc. Rev. 27*, 453–460.

(20) Peskin, A. V., Midwinter, R. G., Harwood, D. T., and Winterbourn, C. C. (2004) Chlorine transfer between glycine, taurine and histamine: Reaction rates and impact on cellular reactivity. *Free Radical Biol. Med. 37*, 1622–1630.

(21) Peskin, A. V., and Winterbourn, C. C. (2006) Taurine chloramine is more selective than hypochlorous acid at targeting critical cysteines and inactivating creatine kinase and glyceraldehyde-3-phosphate dehydrogenase. *Free Radical Biol. Med. 40*, 45–53.

(22) Summers, F. A., Morgan, P. E., Davies, M. J., and Hawkins, C. L. (2008) Identification of plasma proteins that are susceptible to thiol oxidation by hypochlorous acid and *N*-chloramines. *Chem. Res. Toxicol. 21*, 1832–1840.

(23) Bergt, C., Fu, X., Huq, N. P., Kao, J., and Heinecke, J. W. (2004) Lysine residues direct the chlorination of tyrosines in YxxK motifs of apolipoprotein A-I when hypochlorous acid oxidizes HDL. *J. Biol. Chem. 279*, 7856–7866.

(24) Hawkins, C. L., Pattison, D. I., and Davies, M. J. (2003) Hypochlorite-induced oxidation of amino acids, peptides and proteins. *Amino Acids 25*, 259–274.

(25) Hawkins, C. L., and Davies, M. J. (1998) Hypochlorite-induced damage to proteins: Formation of nitrogen-centred radicals from lysine residues and their role in protein fragmentation. *Biochem. J. 332*, 617–625.

(26) Hawkins, C. L., Rees, M. D., and Davies, M. J. (2002) Superoxide radicals can act synergistically with hypochlorite to induce damage to proteins. *FEBS Lett. 510*, 41–44.

(27) Rees, M. D., Hawkins, C. L., and Davies, M. J. (2004) Hypochlorite and superoxide radicals can act synergistically to induce fragmentation of hyaluronan and chondritin sulfates. *Biochem. J. 381*, 175–184.

(28) Chapman, A. L., Skaff, O., Senthilmohan, R., Kettle, A. J., and Davies, M. J. (2009) Hypobromous acid and bromamine production by neutrophils and modulation by superoxide. *Biochem. J. 417*, 773–781.

(29) Hawkins, C. L., and Davies, M. J. (2005) The role of reactive N-bromo species and radical intermediates in hypobromous acid-induced protein oxidation. *Free Radical Biol. Med. 39*, 900–912.

(30) Lind, J., Shen, X., Eriksen, T. E., Merenyi, G., and Eberson, L. (1991) One-electron reduction of N-bromosuccinimide. Rapid expulsion of a bromine atom. *J. Am. Chem. Soc. 113*, 4629–4633.

(31) Baumgartner, M. T., and Foray, S. G. (2003) A theoretical study of nitrogen radicals. Generation, reactivity and selectivity in electron transfer reactions. *J. Mol. Struct. (Theochem) 633*, 7–14.

(32) Peskin, A. V., and Winterbourn, C. C. (2001) Kinetics of the reactions of hypochlorous acid and amino acid chloramines with thiols, methionine, and ascorbate. *Free Radical Biol. Med. 30*, 572–579.

(33) Prutz, W. A. (1999) Consecutive halogen transfer between various functional groups induced by reaction of hypohalous acids: NADH oxidation by halogenated amide groups. *Arch. Biochem. Biophys. 371*, 107–114.

(34) Fridovich, I. (1995) Superoxide radical and superoxide dismutases. *Annu. Rev. Biochem. 64*, 97–112.

(35) Morris, J. C. (1966) The acid ionization constant of HOCl from 5 to 35 °C. *J. Phys. Chem. 70*, 3798–3805.

(36) Eyer, P., Worek, F., Kiderlen, D., Sinko, G., Stuglin, A., Simeon-Rudolf, V., and Reiner, E. (2003) Molar absorption coefficients for the reduced Ellman reagent: reassessment. *Anal. Biochem. 312*, 224–227.

(37) Pattison, D. I., Davies, M. J., and Asmus, K.-D. (2002) Absolute rate constants for the formation of nitrogen-centred radicals from chloramines/amides and their reactions with antioxidants. *J. Chem. Soc., Perkin Trans. 2*, 1461–1467.

(38) Anderson, R. F., Denny, W. A., Li, W., Packer, J. E., Tercel, M., and Wilson, W. R. (1997) Pulse radiolysis studies on the fragmentation of arylmethyl quaternary nitrogen mustards by one-electron reduction in aqueous solution. *J. Phys. Chem. A 101*, 9704–9709.

(39) Mulazzani, Q. G., Dangelantonio, M., Venturi, M., Hoffman, M. Z., and Rodgers, M. A. J. (1986) Interaction of formate and oxalate ions with radiation-generated radicals in aqueous solution - methylviologen as a mechanistic probe. *J. Phys. Chem. 90*, 5347–5352.

(40) Kettle, A. J., Anderson, R. F., Hampton, M. B., and Winterbourn, C. C. (2007) Reactions of superoxide with myeloperoxidase. *Biochemistry 46*, 4888–4897.

(41) Hehre, W. J., Radom, L., Schleyer, P. v. R., and Pople, J. A. (1986) *Ab Initio Molecular Orbital Theory*, Wiley, New York.

(42) Jensen, F. (2006) *Introduction to Computational Chemistry*, 2nd ed., Wiley, Chichester.

(43) Koch, W., and Holthausen, M. C. (2001) *A Chemist's Guide to Density Functional Theory*, 2nd ed., Wiley-VCH, New York.

(44) Frisch, M. J., Trucks, G. W., Schlegel, H. B., Scuseria, G. E., Robb, M. A., Cheeseman, J. R., Montgomery, J., J., A., Vreven, T., Kudin, K. N., Burant, J. C., Millam, J. M., Iyengar, S. S., Tomasi, J., Barone, V., Mennucci, B., Cossi, M., Scalmani, G., Rega, N., Petersson, G. A., Nakatsuji, H., Hada, M., Ehara, M., Toyota, K., Fukuda, R., Hasegawa, J., Ishida, M., Nakajima, T., Honda, Y., Kitao, O., Nakai, H., Klene, M., Li, X., Knox, J. E., Hratchian, H. P., Cross, J. B., Bakken, V., Adamo, C., Jaramillo, J., Gomperts, R., Stratmann, R. E., Yazyev, O., Austin, A. J., Cammi, R., Pomelli, C., Ochterski, J. W., Ayala, P. Y., Morokuma, K., Voth, G. A., Salvador, P., Dannenberg, J. J., Zakrzewski, V. G., Dapprich, S., Daniels, A. D., Strain, M. C., Farkas, O., Malick, D. K., Rabuck, A. D., Raghavachari, K., Foresman, J. B., Ortiz, J. V., Cui, Q., Baboul, A. G., Clifford, S., Cioslowski, J., Stefanov, B. B., Liu, G., Liashenko, A., Piskorz, P., Komaromi, I., Martin, R. L., Fox, D. J., Keith, T., Al-Laham, M. A., Peng, C. Y., Nanayakkara, A., Challacombe, M., Gill, P. M. W., Johnson, B., Chen, W., Wong, M. W., Gonzalez, C., and Pople, J. A. (2004) *Gaussian 03*, revision E.02, Gaussian, Inc., Wallingford, CT.

(45) Frisch, M. J., Trucks, G. W., Schlegel, H. B., Scuseria, G. E., Robb, M. A., Cheeseman, J. R., Scalmani, G., Barone, V., Mennucci, B., Petersson, G. A., Nakatsuji, H., Caricato, M., Li, X., Hratchian, H. P., Izmaylov, A. F., Bloino, J., Zheng, G., Sonnenberg, J. L., Hada, M., Ehara, M., Toyota, K., Fukuda, R., Hasegawa, J., Ishida, M., Nakajima, T., Honda, Y., Kitao, O., Nakai, H., Vreven, T., Montgomery, J., J., A., Peralta, J. E., Ogliaro, F., Bearpark, M., Heyd, J. J., Brothers, E., Kudin, K. N., Staroverov, V. N., Kobayashi, R., Normand, J., Raghavachari, K., Rendell, A., Burant, J. C., Iyengar, S. S., Tomasi, J., Cossi, M., Rega, N., Millam, N. J., Klene, M., Knox, J. E., Cross, J. B., Bakken, V., Adamo, C., Jaramillo, J., Gomperts, R., Stratmann, R. E., Yazyev, O., Austin, A. J., Cammi, R., Pomelli, C., Ochterski, J. W., Martin, R. L., Morokuma, K., Zakrzewski, V. G., Voth, G. A., Salvador, P., Dannenberg, J. J., Dapprich, S., Daniels, A. D., Farkas, Ö., Foresman, J. B., Ortiz, J. V., Cioslowski, J., and Fox, D. J. (2009) *Gaussian 09*, revision A.02, Gaussian, Inc., Wallingford, CT.

(46) Curtiss, L. A., Redfern, P. C., and Raghavachari, K. (2007) Gaussian-4 theory. *J. Chem. Phys. 126*, 084108.

(47) Merrick, J. P., Moran, D., and Radom, L. (2007) An evaluation of harmonic vibrational frequency scale factors. *J. Phys. Chem. A 111*, 11683–11700.

(48) Barone, V., and Cossi, M. (1998) Quantum calculation of molecular energies and energy gradients in solution by a conductor solvent model. *J. Phys. Chem. A 102*, 1995–2001.

(49) Cossi, M., Rega, N., Scalmani, G., and Barone, V. (2003) Energies, structures, and electronic properties of molecules in solution with the C-PCM solvation model. *J. Comput. Chem. 24*, 669–681.

(50) Takano, Y., and Houk, K. N. (2005) Benchmarking the conductor-like polarizable continuum model (CPCM) for aqueous solvation free energies of neutral and ionic organic molecules. *J. Chem. Theory Comput. 1*, 70–77.

(51) Reiss, H., and Heller, A. (1985) The absolute potential of the standard hydrogen electrode - a new estimate. *J. Phys. Chem. 89*, 4207–4213.

(52) Thomas, E. L., Bozeman, P. M., Jefferson, M. M., and King, C. C. (1995) Oxidation of bromide by the human leukocyte enzymes myeloperoxidase and eosinophil peroxidase. Formation of bromamines. *J. Biol. Chem. 270*, 2906–2913.

(53) Buxton, G. V., and Sellers, R. M. (1973) Acid dissociation constant of the carboxyl radical. Pulse radiolysis studies of aqueous solutions of formic acid and sodium formate. *J. Chem. Soc., Faraday Trans. 1 69*, 555–559.

(54) Neta, P., Simic, M., and Hayon, E. (1969) Pulse radiolysis of aliphatic acids in aqueous solutions. I. Simple monocarboxylic acids. *J. Phys. Chem. 73*, 4207–4213.

(55) Lind, J., Jonsson, M., Eriksen, T. E., Merenyi, G., and Eberson, L. (1993) One-electron reduction potential and ring opening of the succinimidyl radical in water. *J. Phys. Chem. 97*, 1610–1614.

(56) Johnson, H. D., Cooper, W. J., Mezyk, S. P., and Bartels, D. M. (2002) Free radical reactions of monochloramine and hydroxylamine in aqueous solution. *Radiat. Phys. Chem. 65*, 317–326.

(57) Poskrebyshev, G. A., Huie, R. E., and Neta, P. (2003) Radiolytic reactions of monochloramine in aqueous solutions. *J. Phys. Chem. A 107*, 7423–7428.

(58) Canle, M. L., Santaballa, J. A., and Steenken, S. (1999) Photo- and radiation-chemical generation and thermodynamic properties of the aminium and aminyl radicals derived from *N*-Phenylglycine and (*N*-Chloro,*N*-phenyl) glycine in aqueous solution: evidence for a new photoionization mechanism for aromatic amines. *Chem.—Eur. J. 5*, 1192–1201.

(59) Hayon, E., and Simic, M. (1971) Pulse radiolysis study of cyclic peptides in aqueous solution. Absorption spectrum of the peptide radical -NHCHCO-. *J. Am. Chem. Soc. 93*, 6781–6786.

(60) Radisic, D., Xu, S. J., and Bowen, K. H. (2002) Photoelectron spectroscopy of the anions, CH_3NH^- and $(CH_3)_2N^-$ and the anion complexes, $H^-(CH_3NH_2)$ and $(CH_3)_2N^-[(CH_3)_2NH)]$. *Chem. Phys. Lett. 354*, 9–13.

(61) Wickham-Jones, C. T., Ervin, K. M., Ellison, G. B., and Lineberger, W. C. (1989) NH_2 electron affinity. *J. Chem. Phys. 91*, 2762–2763.

(62) Ervin, K. M., Anusiewicz, W., Skurski, P., Simons, J., and Lineberger, W. C. (2003) The only stable state of O_2^- is the X $^2\Pi_g$ ground state and it (still!) has an adiabatic electron detachment energy of 0.45 eV. *J. Phys. Chem. A 107*, 8521–8529.

(63) Gianola, A. J., Ichino, T., Hoenigman, R. L., Kato, S., Bierbaum, V. M., and Lineberger, W. C. (2005) Photoelectron spectra and ion chemistry of imidazolide. *J. Phys. Chem. A 109*, 11504–11514.

(64) Blondel, C., Cacciani, P., Delsart, C., and Trainham, R. (1989) High-resolution determination of the electron-affinity of fluorine and bromine using crossed ion and laser-beams. *Phys. Rev. A 40*, 3698–3701.

(65) Martin, J. D. D., and Hepburn, J. W. (1998) Determination of bond dissociation energies by threshold ion-pair production spectroscopy: An improved D_0(HCl). *J. Chem. Phys. 109*, 8139–8142.

(66) Wood, G. P. F., Henry, D. J., and Radom, L. (2003) Performance of the RB3-LYP, RMP2, and UCCSD(T) procedures in calculating radical stabilization energies for •NHX radicals. *J. Phys. Chem. A 107*, 7985–7990.

(67) Rao, P. S., Metz, H. N., Wilson, D. W., and Hayon, E. M. (1997) One-electron reduction reactions of some inorganic nitrogen radicals in water. *Indian J. Chem., Sect. A 36*, 649–656.

(68) Merenyi, G., Lind, J., and Eberson, L. (1998) The return of the succinimidyl radical. *Acta Chem. Scand. 52*, 62–66.

(69) Walling, C., El-Taliawi, G. M., and Zhao, C. (1983) Radical chain carriers in N-bromosuccinimide brominations. *J. Am. Chem. Soc. 105*, 5119–5124.

(70) Skell, P. S., Tlumak, R. L., and Seshadri, S. (1983) Selectivities of π- and σ-succinimidyl radicals in substitution and addition reactions. Appendix. Response to Walling, El-Taliawi and Zhao. *J. Am. Chem. Soc. 105*, 5125–5131.

(71) Lind, J., Jonsson, M., Xinhua, S., Eriksen, T. E., Merenyi, G., and Eberson, L. (1993) Kinetics of radical-initiated chain bromination of 2-methyl-2-propanol by N-bromosuccinimide in water. *J. Am. Chem. Soc. 115*, 3503–3510.

(72) Koppenol, W. H., Stanbury, D. M., and Bounds, P. L. (2010) Electrode potentials of partially reduced oxygen species, from dioxygen to water. *Free Radical Biol. Med. 49*, 317–322.

(73) Henderson, J. P., Byun, J., Takeshita, J., and Heinecke, J. W. (2003) Phagocytes produce 5-chlorouracil and 5-bromouracil, two mutagenic products of myeloperoxidase, in human inflammatory tissue. *J. Biol. Chem. 278*, 23522–23528.

(74) Takeshita, J., Byun, J., Nhan, T. Q., Pritchard, D. K., Pennathur, S., Schwartz, S. M., Chait, A., and Heinecke, J. W. (2006) Myeloperoxidase generates 5-chlorouracil in human atherosclerotic tissue. A potential pathway for somatic mutagenesis by macrophages. *J. Biol. Chem. 281*, 3096–3104.

(75) Lentner, C., Ed. (1984) *Geigy Scientific Tables: Physical Chemistry, Composition of Blood, Hematology, Somatometric Data*, Vol. 3, Ciba-Geigy Ltd., Basle, Switzerland.

(76) Winterbourn, C. C., Hampton, M. B., Livesey, J. H., and Kettle, A. J. (2006) Modeling the reactions of superoxide and myeloperoxidase in the neutrophil phagosome: implications for microbial killing. *J. Biol. Chem. 281*, 39860–39869.